¹H NMR Characterization of Myoglobins Where Exogenous Ligands Replace the Proximal Histidine[†]

Sean M. Decatur and Steven G. Boxer*

Department of Chemistry, Stanford University, Stanford, California 94305-5080

Received September 6, 1994; Revised Manuscript Received December 8, 1994[®]

ABSTRACT: The role of the proximal ligand in determining the structure and ligand binding properties of sperm whale myoglobin has been investigated using the mutant H93G(L), where the proximal histidine has been replaced with glycine, creating a cavity which can be occupied by a variety of exogenous ligands, L, to the iron [Barrick, D. (1994) *Biochemistry 33*, 6546−6554; DePillis, G. D., Decatur, S. M., Barrick, D., & Boxer, S. G. (1994) *J. Am. Chem. Soc. 116*, 6981−6982]. In this report, we present the assignments of selected protons of the heme and heme pocket residues in the metcyano complexes of H93G with Im and a series of methyl-substituted Ims [H93G(Im)CN, H93G(N-MeIm)CN, H93G(2-MeIm)CN, H93G-(4-MeIm)CN]. Each complex has a unique ¹H NMR spectrum, providing a fingerprint for documenting the ligand exchange phenomenon. Moreover, the identification of NOEs between the protons of proximal ligands and protons of proximal pocket amino acid residues confirms that the new ligand occupies the proximal cavity in solution. The pattern of hyperfine-shifted heme methyl resonances in H93G(Im)CN is very different from that of wild-type Mb, consistent with the differences compared to wild-type in orientation of the proximal imidazole observed in the X-ray crystal structure of H93G(Im) [Barrick, D. (1994) *Biochemistry 33*, 6546−6554]. Addition of deuterated Im to H93G(Im)CN permits direct observation of exchange of proximal ligands with ligands from solution; exchange of Im for deuterated Im in the metcyano complex occurs with half-life of around 10 min. The heme methyl pattern is very similar in the series of H93G(MeIm) complexes, suggesting that the orientation of the imidazole is similar in these proteins. While Im and 4-MeIm have the same affinity for the proximal binding site, N-MeIm and 2-MeIm bind more weakly than Im in the metcyano complex. By characterization of the NMR spectra of these complexes, it is possible to describe interactions between the proximal ligand, the heme, and the protein pocket which play a role in determining the structure and function of the complexes.

Myoglobin (Mb)[1] is extensively studied as a model for exploring the relationship between protein structure, dynamics, and function. Most of this effort has focused on the role of the amino acids in the distal pocket in modulating the kinetics or thermodynamics of ligand binding (Lambright et al., 1989, 1994; Carver et al., 1990; Springer et al., 1994); less is known about the role of the proximal side (Smerdon et al., 1993). As the sole covalent linkage between the polypeptide chain and the iron active site, the proximal histidine (His 93) plays an important yet poorly understood role in determining the functional and spectroscopic properties of the protein. In studies of model compounds, the proximal ligand is easily changed and can be shown to modulate function. For example, subtle changes in the conformation or orientation of the proximal ligand can perturb the kinetics and thermodynamics of the binding of O_2 or other diatomic ligands to the distal side of heme model compounds and proteins (Momenteau & Reed, 1994).

In order to dissect the role of the proximal ligand within the protein, it is desirable to systematically alter the structure,

conformation, and chemistry of the proximal ligand. However, the limited variety of ligands available among the natural amino acids reduces the power of site-directed mutagenesis as a tool to address this problem. The mutants H93C and H93Y have been prepared in human and sperm whale myoglobins (Adachi et al., 1993; Egeberg et al., 1990) and have interesting properties, but there are no amino acids available which can more subtly alter the nature of the proximal ligand. An alternative approach is to remove the covalent linkage with the protein entirely. When the proximal histidine is replaced by glycine and the protein is expressed in *Escherichia coli* in the presence of imidazole, an exogenous imidazole molecule is taken up by the protein and serves as the proximal ligand (Barrick, 1994). Previously, we have reported a method to substitute a wide range of molecules for the proximal imidazole in H93G (DePillis et al., 1994). Using this technique, it is possible to incorporate the diversity of ligands available in model compounds within the Mb matrix. The proteins, H93G(L), where L is the proximal ligand, can be distinguished on the basis of differences in spectroscopic and ligand binding characteristics. Subtle variations in L, such as 1-, 2-, and 4-methyl-substituted imidazoles (Im), can be used to systematically explore the effects of steric bulk, structure, and basicity of the proximal ligand on protein function.

¹H NMR spectroscopy of metcyano complexes of heme proteins and model compounds is useful for characterizing both the protein structure and heme electronic structure.

---

[1] Abbreviations: Mb, myoglobin; MbCN, metcyanomyoglobin; WT, wild type; SW, sperm whale; L, exogenous ligand; Im, imidazole; MeIm, methyl-substituted imidazole; NMR, nuclear magnetic resonance; NOE, nuclear overhauser effect; FID, free induction decay.

A

His 64

Phe 43

Val 68

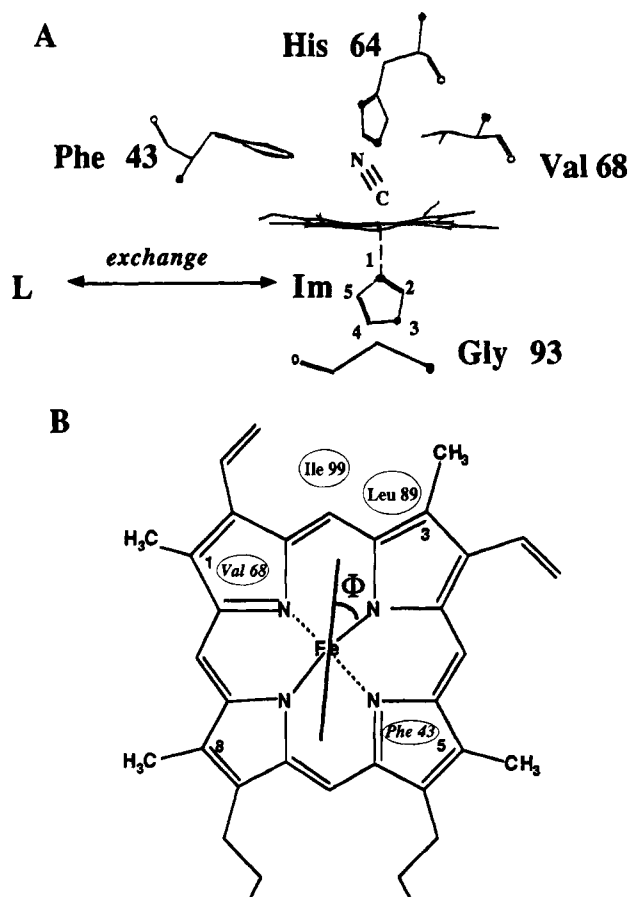**L** ⟶ *exchange* ⟶ **Im**

Gly 93

B

FIGURE 1: (A) Schematic diagram of the heme pocket in H93G-(Im)CN. The proximal Im undergoes exchange with exogenous ligands (L) from solution. (B) Projection of the Im plane onto the heme plane. The angle Φ between the Im projection and the N_{IV}–Fe–N_{II} plane is about 10° in WT SWMb, with His 93 nearly eclipsing the heme pyrrolic nitrogens (Takano, 1977). In H93G-(Im), the angle is closer to 45°, and the Im projection is aligned with the *meso* carbons of the heme (Barrick, 1994). Positions of important amino acids are indicated by circles; italicized labels indicate distal pocket residues [following Kendrew (1962)].

Metcyano complexes of hemes are low spin ($S = \frac{1}{2}$), paramagnetic species; in heme proteins, contact and dipolar shifts experienced by the heme and neighboring amino acids produce spectra with a large dispersion of resonances, facilitating the assignment process. Furthermore, the pattern of hyperfine-shifted resonances of the heme is characteristic of the electronic asymmetry in the heme produced by interactions with the anisotropic protein environment (La Mar, 1979) and by the orientation of the axial ligands (Traylor & Berzinis, 1980; Yamamoto et al., 1990). Small but systematic changes in the heme methyl chemical shifts are observed upon mutation of amino acids of the distal pocket (Adachi et al., 1991; Rajaratham et al., 1994), but larger changes are observed upon alteration of the proximal ligand. Yamamoto and co-workers have correlated the pattern of hyperfine-shifted resonances of the heme methyl protons with the angle Φ between the projection of the proximal imidazole on the plane of the heme and the N_{II}–Fe–N_{IV} axis (Figure 1). In addition, we have demonstrated that substituting the proximal ligand in H93G(L)CN produces new complexes which have unique and distinguishable NMR spectra (DePillis et al., 1994). These changes in spectral features provide a window for observing the kinetic and thermodynamic properties of proximal ligand exchange for

relatively conservative substitutions. In subsequent papers, we will describe the properties of other spin and distal ligation states as well as more drastic changes in the proximal ligand.

MATERIALS AND METHODS

Protein Preparation. The expression and purification of sperm whale Mb mutant H93G(Im) has been described in detail elsewhere (Barrick, 1994). The proximal ligand in H93G can be exchanged by a simple diafiltration procedure (DePillis et al., 1994). An excess (10−100-fold) of the new ligand is added to a concentrated stock of H93G(Im). After several successive concentrations and redilutions in a Centricon-10 (Amicon), the concentration of excess ligand L was reduced to about 1 mM.

^{1}H NMR samples were prepared in either D_2O or 90% $H_2O/10\%$ D_2O buffers containing 0.1 M potassium phosphate, 10 mM KCN, and 1 mM proximal ligand L. The uncorrected pH of the samples was either 7.0 (D_2O) or 9.4 (90% H_2O). Protein concentrations were typically between 1 and 3 mM.

Reconstitution with 1-CD₃ Protohemin IX. The apoprotein of H93G was prepared by the standard 2-butanone extraction method (Teale, 1959). 1-CD₃ protohemin-IX was a generous gift of Dr. Kevin Smith. A 5% excess of the heme dissolved in 0.1 N NaOH was added dropwise to the apoprotein solution containing 10 mM Im. The solution was passed through a PD-10 column (Pharmacia) to remove unbound heme. Reconstituted H93G(Im) was kept at room temperature for 12 h to allow heme reorientation equilibration to occur[2] and then prepared as an NMR sample as described above.

¹H NMR Experiments. All ^{1}H NMR spectra were collected on a GE Omega 500 MHz spectrometer. Spectra were routinely measured at 30 °C. The residual water resonance was saturated with the decoupler channel during the predelay period.

Steady-state 1D NOE difference spectra were obtained with a saturation time of 100 ms and mixing time of 1 ms. The delay between acquisitions was set to 700 ms. Typically, 9600 scans alternating on- and off-resonance consisting of 2048 points over a spectral window of 25 000−30 000 Hz were collected. The repetition rate was about 1 Hz. Difference FIDs were apodized with 5−10 Hz line broadening and zero-filled to 4096 points before Fourier transformation.

---

[2] When apomyoglobin is reconstituted with heme, initially two heme conformers (related by 180° rotation about the heme $\alpha-\gamma$ axis) are present; equilibrium is reached after several hours. The reorientation of the heme between these two conformers has been extensively characterized by La Mar and co-workers (La Mar et al., 1989; Hauksson et al., 1990). When Mb is reconstituted with protoporphyrin IX, which lacks the Fe and therefore a covalent linkage between prosthetic group and protein, the equilibrium heme conformation is observed within 20 min after reconstitution, suggesting that either His 93−iron bond formation is criticial in causing metastable heme disorder or that bond breakage and formation is the rate limiting step in heme reorientation (La Mar et al., 1989). Because the prosthetic group in H93G(Im) is not attached to the polypeptide chain, heme reorientation kinetics may occur on an intermediate time scale, and it might be a valuable tool in distinguishing between the two mechanisms. For the purpose of the present study, the spectrum of reconstituted H93G(Im) after a 12 h waiting period was indistinguishable from that of protein isolated from *E. coli*.

Absolute value COSY (MCOSY) and phase-sensitive NOESY spectra were collected following published protocols for optimizing collection of spectra for paramagnetic met-cyano—heme protein complexes (Alam & Satterlee, 1994; La Mar & de Ropp, 1993; Emerson & La Mar, 1990). MCOSY spectra were collected over spectral widths of 15 000—20 000 Hz. A total of 1024 t_2 points and 512 t_1 blocks were collected. For NOESY spectra, 1024 t_1 points and 256 t_2 blocks were collected with a spectral width of 25 000 Hz and a mixing time of 100 ms. 2D data sets were processed using the program FTNMR (Hare Research). Data were apodized with a skewed-squared sine bell function in both dimensions and zero-filled to 2048 × 2048 points.

T_1 values for selected protons were measured using a standard inversion—recovery sequence. Plots of $\log[(I_\infty - I(t))/2I_\infty]$ vs τ in paramagnetic complexes have curvature due to contributions from cross-relaxation (Sletten et al., 1983). However, in spin $^1/_2$ metcyano—heme protein complexes, the initial slopes of the plots of $\log[(I_\infty - I(t))/2I_\infty]$ vs τ have been used to determine reasonably accurate values of T_1 (La Mar & de Ropp, 1993). The distance between the proton and the iron (R_{Fe}) can be calculated from the relationship (La Mar & de Ropp, 1993)

$$(R_{Fe}^i/R_{Fe}^j) = (T_1^i/T_1^j)^{1/6} \quad (1)$$

Heme methyl protons are ~6.1 Å from the Fe; however, it has been shown that scalar relaxation makes an increasing contribution to T_1 of heme methyl protons whose chemical shifts are >15 ppm (Cutnell et al., 1981). Thus, we have chosen the T_1 of the most upfield of the assigned heme methyl protons, the 1-Me, as a standard to determine the R_{Fe} of other resonances. For comparison R_{Fe} values were also calculated from coordinates of the X-ray structure of H93G(Im)H$_2$O (Barrick, 1994). The SUPERWEFT sequence (Inubushi & Becker, 1983) was used to enhance resonances from fast-relaxing protons relative to the slowly relaxing diamagnetic envelope.

RESULTS

The ^{1}H NMR spectra of WT and H93G(Im) are aligned for comparison in Figure 2. Although there are many differences in the peak positions of the H93G(Im)CN spectrum compared to that of WT MbCN, the general features of the spectrum, including dispersion of resonances (~26 to −7 ppm in H93G; 28 to −10 ppm in WT) and sample homogeneity, are similar. Assignments for the spectra are listed in Table 1. Resonances were assigned using a combination of 1D and 2D data and isotopic substitution. The extensive assignments in WT SWMb (Emerson & La Mar, 1990), as well as the crystal structure of the metaquo form of H93G(Im), were helpful guides in the process.

Assignment of Heme 1-Me and 8-Me Groups. The resonance for the heme 1-Me group was readily assigned by reconstitution of H93G(Im) with 1-CD$_3$ protohemin-IX, as the peak at 16.7 ppm disappears in this complex (Figure 3B). Furthermore, this resonance has an NOE with the methyl resonance at 25.6 ppm (Figure 3C). There is also a cross peak between these resonances in the 2D NOESY spectrum (data not shown). Since the 1-Me and 8-Me groups of the heme are the only methyl groups close enough for
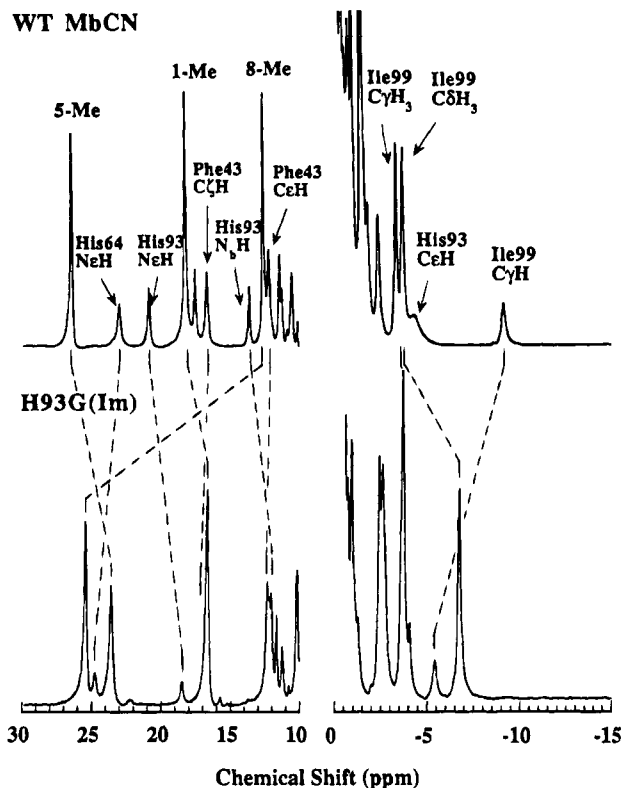

FIGURE 2: ^{1}H NMR spectra of WT MbCN and H93G(Im)CN in 90% H$_2$O, pH 9.4, 30 °C. Assignments are listed in Table 1.

Table 1: ^{1}H Chemical Shift Assignments for H93G(Im)CN

proton	δ (ppm)	T_1 (ms)	R_{Fe} (Å)[a]	R_{Fe} (Å)[b]
heme				
8-Me	25.6	60	c	6.1
5-Me	23.6	100	c	6.1
1-Me	16.7	130		6.1
2-α	11.4	115	6.0	5.9
2-β	−0.34	d	d	6.1−6.9
	0.48	d	d	
4-α	10.2	d	d	5.9
4-β	−3.88	140	6.3	6.1−6.9
	−2.54	170	6.5	
Im				
C4H	12.1	30	4.8	4.5
NH	18.7	d	d	4.4
Ile 99				
CβH	0.28	d	d	6.2−7.0
CγH	−5.33	70	5.6	6.3−6.7
	−3.67	85	5.8	
CγH$_3$	−3.48	90	5.8	6.1
CδH$_3$	−6.68	40	5.1	5.8
Gly 93				
CαHs	6.77	d	d	6.0
N$_{bH}$	12.2	d	d	5.2
Phe 43				
CδHs	8.57	d	d	6.9, 8.5
CεHs	12.4	70	5.6	4.7, 6.7
CζH	16.9	70	5.6	4.49
His 64				
NεH	24.8	d	d	3.71

[a] Calculated using eq 1. [b] Taken from X-ray coordinates of H93G(Im)H$_2$O (Barrick, 1994). [c] Contact shift makes application of eq 1 invalid. [d] Not measured because of overlapping resonances.

observing an NOE connectivity, the resonance at 25.6 ppm can be assigned to the heme 8-CH$_3$ group (Emerson & La Mar, 1990).

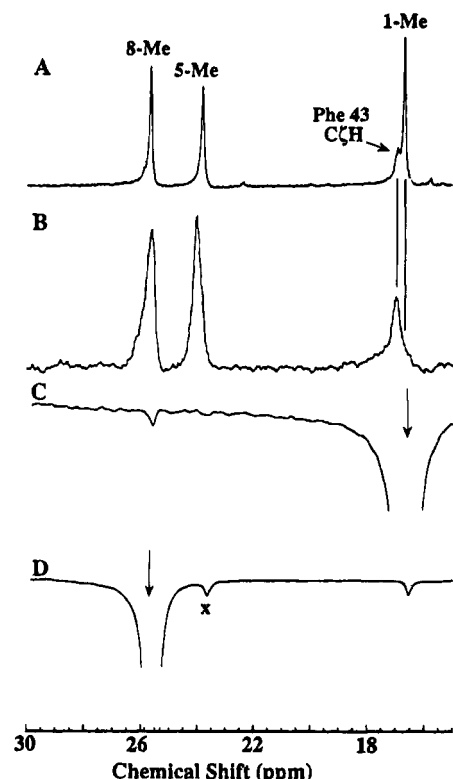*Assignment of Other Heme Protons.* The spin systems for the heme vinyl groups are readily identifiable in the

FIGURE 3: (A) ^{1}H NMR spectra of H93G(Im)CN in D_2O buffer, pH 7.0. (B) H93G(Im)CN reconstituted with 1-CD$_3$ protohemin. The methyl peak at 16.7 ppm has disappeared. (C) NOE difference spectra of H93G(Im)CN upon saturation of the resonance at 16.7 ppm. A small NOE is detected at 25.6 ppm. (D) NOE difference spectra upon saturation of 25.6 ppm. A small NOE is seen at 16.7 ppm. The peak marked with "x" is due to decoupler overflow.

MCOSY spectra. Cross peaks are seen between the resonance at 11.43 ppm and resonances at 0.50 and −0.34 ppm (Figure 4, peaks 1 and 2). Because NOEs and NOESY cross peaks between these protons and the nearby 1-Me group are observed, these are assigned to the heme 2-α and the 2-β protons. The T_1 for the 11.4 ppm resonance, ∼115 ms, is also consistent with the R_{Fe} expected of the 2-α H (see Table 1). A similar pattern of MCOSY cross peaks is also observed between the peaks at 10.2 and −2.54 and −3.88 ppm (peaks 3 and 4). These peaks have been assigned to the heme 4-α and 4-β protons. T_1 and R_{Fe} data also support these assignments. The methyl resonance at 23.4 ppm has been assigned to the heme 5-Me group on the basis of NOEs to the 4-α proton and the CδHs of Phe 43 (see below).

Assignment of Resonances of Ile 99. The dipolar shifted resonances of Ile 99 protons appear in the upfield hyperfine shifted region and are readily assigned from the MCOSY spectra (Figure 4B). Cross peaks are observed between the CδH$_3$ protons at −6.7 ppm and the two geminal CγHs at −5.33 and −3.67 ppm (Figure 4B, cross peaks 5 and 6). 1D NOEs have been observed between these protons. Saturation at −5.33 ppm gives a very large NOE to −3.67 ppm, which is expected for a geminal pair of protons in the 1D NOE spectra (data not shown). There is an additional cross peak (7) between resonances at −3.67 and 0.28 ppm. The resonance at 0.28 ppm has been assigned to the CβH; this resonance also has a cross peak with a methyl resonance at −3.48 ppm, which can be assigned to the CγH$_3$ (8). Intra-side-chain NOEs between CδH$_3$ and the CγHs and CγH and the CβH have been observed in both the NOESY spectrum and 1D NOE spectra. Saturation of the 5-Me resonance also
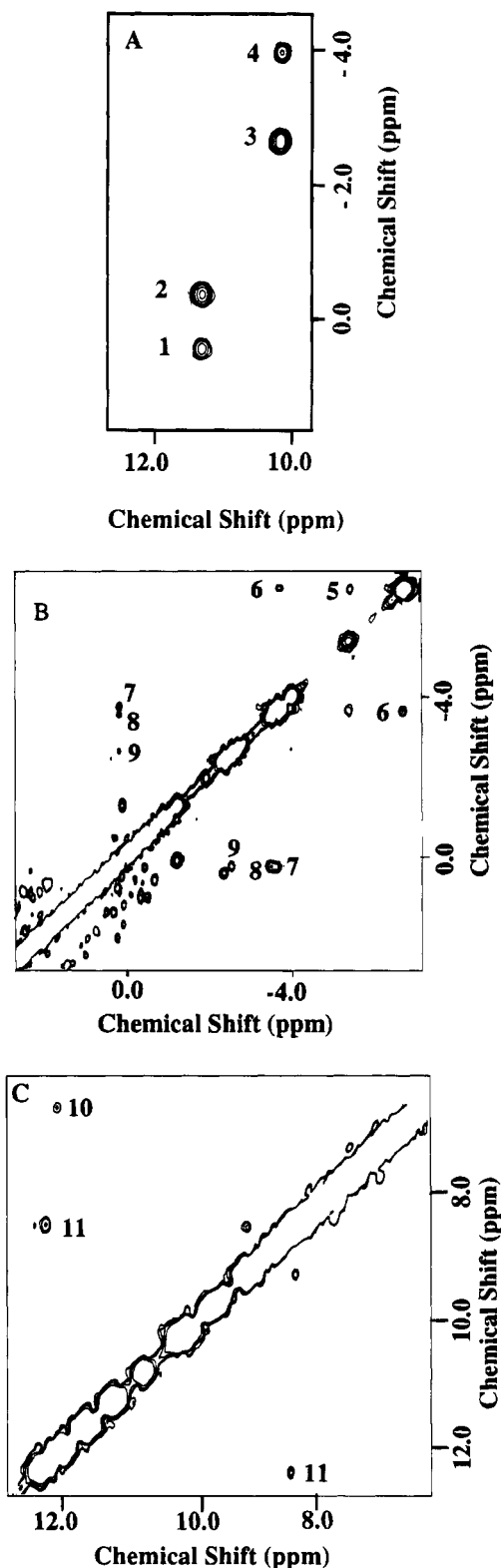

FIGURE 4: MCOSY spectra of H93G(Im)CN in D_2O buffer, pH 7.0, 30 °C. (A) Region containing cross peaks of the heme vinyl groups. (B) Upfield region containing cross peaks for Ile 99 protons. (C) Aromatic region of the spectrum, with cross peaks for Phe 43 and Gly 93.

gives a small but reproducible NOE at −6.67 ppm, the CδH$_3$ of Ile 99, as seen in the WT protein (Ramaprasad et al., 1984).

Assignment of Gly 93 Protons. An exchangeable proton at 12.2 ppm has been assigned to the amide NH of Gly 93 on the basis of comparisons to the WT protein (in which
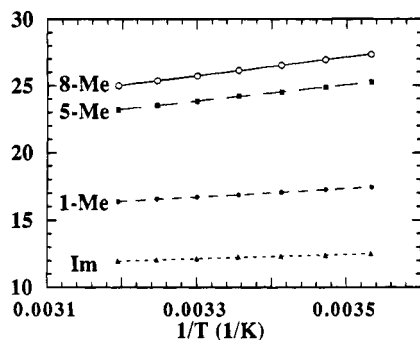
FIGURE 5: Temperature dependence of the chemical shifts of heme methyl protons and Im C4H in H93G(Im)CN.

the His 93 backbone NH has a resonance at 13.2 ppm). This proton also has an NOE to the Im NH. In the MCOSY spectrum, there is a cross peak between this resonance and a resonance at 6.7 ppm, which can be assigned to one (or both) of the CαH protons of Gly 93 (Figure 4B, cross peak 5).

Assignment of Phe 43 Protons. In the spectrum of WT MbCN, the protons of Phe 43 can be identified on the basis of their short T_1 values, NOEs with the heme 5-Me, and characteristic COSY cross peaks. Also, the CδH (8.70 ppm) and both CεH (12.58 ppm) give only one resonance, each integrating for two protons (Emerson et al., 1988). In the spectrum of H93G(Im)CN, the resonance at 12.4 ppm integrates for two protons with $T_1 < 80$ ms. The only indistinguishable pair of protons which are this close to the iron on Phe 43, either the CδHs or CεHs. Figure 4B shows the aromatic region of the MCOSY spectrum; a cross peak is observed at (12.4, 8.57; no. 6). When the 5-Me resonance is saturated, NOEs can be observed at 16.9, 12.4, and 8.57 ppm (data not shown). On the basis of these data and comparisons with the assignments in WT, we assign the CδH protons to 8.57 ppm, with the CεH protons at 12.4 ppm and the CζH at 16.9 ppm. No COSY cross peak has been observed between the 16.9 ppm resonance and either the 12.4 or 8.57 ppm resonances, likely because of the short T_1s of the protons (La Mar & de Ropp, 1993). These assignments are very similar to the Phe 43 protons of WT MbCN, where the CδHs, CεHs, and CζH have been assigned to 8.70, 12.58, and 17.27 ppm respectively (Emerson & La Mar, 1990).

Temperature Dependence of H93G(Im) Resonances. Paramagnetically shifted chemical shifts should have a linear dependence on $(1/T)$ in accordance with the Curie relationship (La Mar & Walker, 1979; Walker & Simonis, 1993). ^{1}H spectra were collected at temperatures over the range 10−40 °C, and the chemical shifts of heme methyl resonances are plotted vs $(1/T)$ in Figure 5. The expected linear relationships are observed.

Assignment of Proximal Im Protons. A resonance at 12.1 ppm is readily assigned to the proximal Im by exchange of Im for deuterated Im (Im-d_3) (Figure 6A). With a T_1 of ~70 ms, the R_{Fe} determined by eq 1 is ~5.56 Å; only the Im C4 is this far away from the Fe, so this resonance can be assigned to the Im C4H. The resonance at 18.7 ppm (see Figure 2) gives an NOE to 12.1 ppm. This peak is exchanged out in D_2O (Figure 3A); we assign this resonance to the exchangeable NH of the Im. The Im C2H and the C5H protons should give very broad resonances due to their close proximity to the Fe (less than 3 Å), and resonances for these protons have not yet been located. Because the
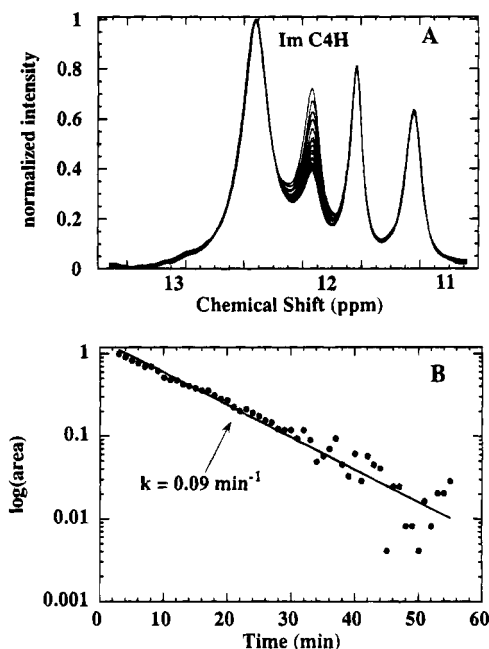

FIGURE 6: (A) Change in NMR spectra of H93G(Im)CN upon addition of deuterated Im to the solution. While the amplitudes and areas of the other peaks in this region remain constant, the Im C4H resonance at 12.1 ppm diminishes over time. (B) Time dependence of the area of the C4H resonances at 12.1 ppm, determined by fitting the spectra to a sum of Lorentzian functions.

Im N1−Fe bond is 0.3 Å shorter in H93G(Im) than WT (Barrick, 1994), these peaks are likely more broadened than their WT counterparts.

Kinetics of Proximal Ligand Exchange. When exogenous Im-d_3 is added to a sample of H93G(Im)CN, the amplitude of the C4H resonance at 12.1 ppm decreases over time until equilibrium is reached (Figure 6A). The exchange is completely reversible; addition of an excess of exogenous Im to the same sample can restore the original spectrum (data not shown). Since the exchange process is relatively slow, its kinetics can be directly measured by ^{1}H NMR. Spectra were collected every minute for 1 h after addition of Im-d_3 to a freshly prepared NMR sample containing 1 mM H93G-(Im)CN and 1 mM free Im in solution. The integral of the 12.1 ppm resonance was determined by fitting the region of the spectrum from 13 to 10.7 ppm to a sum of Lorentzian functions. The area of the 12.1 ppm peak decreases over time with exponential kinetics (Figure 6B), with $k = 0.09 \pm 0.01$ min^{-1}. Surprisingly, this rate constant is found to be independent of [Im-d_3] over an order of magnitude (1−20 mM).

Assignments in Methylimidazole (MeIm) Complexes. The downfield hyperfine-shifted region of the ^{1}H spectra of H93G(Im), H93G(N-MeIm), H93G(4-MeIm), and H93G(2-MeIm) are aligned in Figure 7. Each substitued imidazole can be associated with a unique spectrum in the hyperfine-shifted region. Assignments were made by identifying the same MCOSY and NOE connectivities as described above for H93G(Im) as well as reconstitution with 1-CD$_3$ hemin. One significant difference in these spectra is the presence of an additional methyl resonances in the downfield hyperfine-shifted region. These resonances have T_1 values shorter than that expected for a heme methyl group; on the basis of these data, we have assigned these resonances to the methyl substituents on the imidazole ring. Upon saturation of the
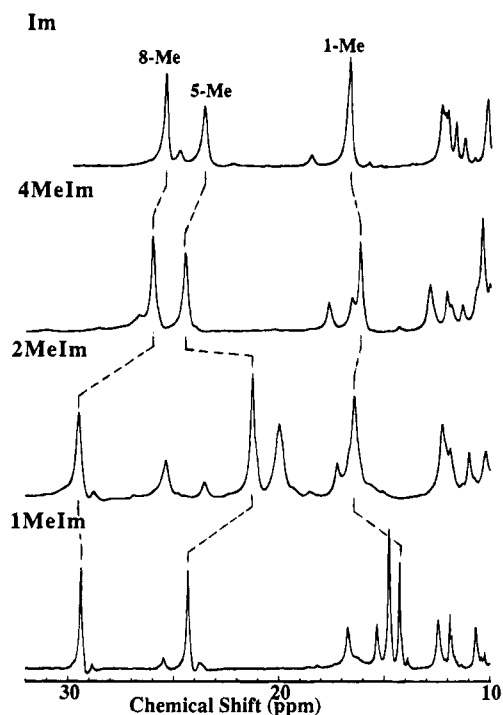
FIGURE 7: Downfield hyperfine-shifted region of the ^{1}H NMR spectra of H93G(MeIm)CN in 90% H_2O, pH 9.4, 30 °C. Assignments are listed in Table 2.
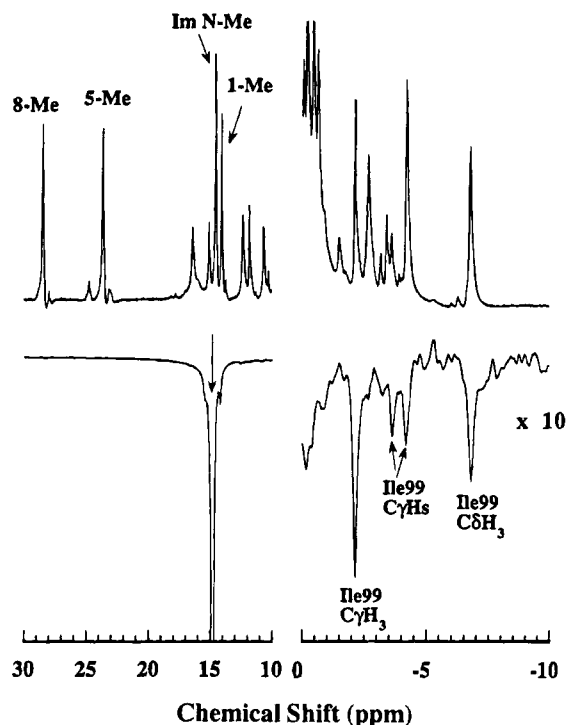

FIGURE 8: NOE difference spectrum of H93G(N-MeIm)CN, with saturation at the Im 1-CH_3 resonance (14.8 ppm). NOEs to Ile 99 resonances at −6.8, −4.02, and −2.12 ppm are observed.

Table 2: ^{1}H Chemical Shift Assignments for H93G(MeIm)CN

proton	H93G(N-MeIm)	H93G(4-MeIm)	H93G(2-MeIm)
heme			
8-Me	29.6	26.0	29.7
5-Me	24.4	24.5	21.1
1-Me	14.2	16.18	16.3
2-α	10.7	11.34	9.35
2-β	0.65	0.50	1.06
	−0.12	−0.27	0.43
4-α	9.94	10.03	11.89
4-β	−2.11	−2.59	−2.07
	−3.17	−3.61	−3.27
Im			
N$_b$H		17.7	a
x-Me	14.8	10.4	20.2
Ile 99			
CβH	0.72	0.20	0.47
CγH	−4.20	−4.45	−4.02
	−3.60	−4.06	−2.78
CγH_3	−2.12	−3.39	−2.34
CδH_3	−6.78	−7.00	−6.54
Gly 93			
N$_b$H	11.8	11.9	a
CαH(s)	6.59	6.58	a
His 64			
NH	25.4	26.7	a
Phe 43			
CζH	16.7	16.7	16.9
CεHs	12.4	12.9	12.3
CδHs	8.57	8.57	a

^{a} Not measured because of overlapping resonances.

ImN-CH_3 resonance (14.8 ppm) in H93G(N-MeIm), an NOE is observed at −6.7 ppm, which has been assigned to the CδH_3 protons of Ile 99 (Figure 8). These data confirm that the "exchanged" ligand occupies the proximal pocket and coordinates the heme iron. Furthermore, the His 64 exchangeable NϵH proton is observable in the H93G(MeIm)-CN spectra.

DISCUSSION

General Spectral Features. The 1D ^{1}H NMR spectrum of H93G(Im)CN, although quite different from that of the WT protein, nonetheless has an overall appearance typical of heme protein metcyano spectra. These features confirm that H93G(Im)CN is a well-defined, stable complex in solution. The observation of a Curie relation between chemical shift and $(1/T)$ over the temperature range 10−40 °C suggests that there is no unusual structural or conformational behavior occurring in H93G(Im)CN compared to WT.

Moreover, ^{1}H NMR of metcyano H93G(L) complexes is a useful tool for documenting and characterizing the ligand exchange phenomenon. Because the chemical shifts of hyperfine-shifted heme resonances are sensitive to subtle perturbations in ligand conformation, the downfield region of the spectrum is a fingerprint for each proximal ligand. The observation of NOEs between the proximal ligand (such as N-MeIm and 4-MeIm) and amino acids of the proximal side (such as Ile 99) unambiguously confirms that ligand replacement occurs on the proximal side of the heme. This structural data, available through routine ^{1}H NMR, is a valuable complement to the functional fingerprint of each ligand observed by measurement of CO recombination (DePillis et al., 1994), creating a powerful methodology for examining structure/function questions involving the proximal ligand.

Orientation of Ile 99. The chemical shifts and T_1 values for the CδH_3, CγHs, and CγH_3 of Ile 99 in H93G(Im) differ from those observed in WT MbCN (Table 1). These differences are consistent with the observation in the crystal structure of H93G(Im) that Ile 99 adopts a different conformation than in WT. Comparison of the coordinates of H93G(Im)H_2O (Barrick, 1994) and WT MbH_2O (Takano, 1977) shows that the CδH_3 and CγH_3 are ~1 Å closer to the Fe in H93G(Im) than in WT. This is consistent with

the observation of shorter T_1's for these protons in the NMR spectrum of H93G(Im)CN. The differences in conformation likely stem from the rotation and tilt of the imidazole ring.

Resonances of Distal Pocket Residues. The assignments for Phe 43 are nearly the same in WT, H93G(Im), and H93G-(MeIm). The conservation of these resonances suggests that the conformation of the distal pocket is not perturbed by the H93G mutation or by proximal ligand substitution. The resonance of the His 64 $N_\epsilon H$ proton is also similar in WT, H93G(Im), and H93G(MeIm). This similarity eliminates the possibility that the distal histidine ligates the Fe in the absence of His 93. Furthermore, the conservation of position of distal pocket resonances is consistent with a proximal, not distal, ligand exchange process.

Conformation of the Imidazole Ring. The plane of the Im observed in the crystal structure of H93G(Im)H₂O (Barrick, 1994) is rotated ~30° relative to that of the histidine in wild-type Mb (Takano, 1977) (Figure 1). The differences between the pattern of heme methyl proton shifts in H93G-(Im)CN and WT MbCN probably reflect these significant changes in the orientation of the proximal ligand. According to the empirical correlations of Yamamoto et al. (1990), the pattern of hyperfine-shifted methyl resonances observed in H93G(Im)CN is qualitatively consistent with the conformation of the Im ring observed in the X-ray crystal structure of H93G(Im)H₂O (Barrick, 1994). Since the heme methyl shift patterns in H93G(MeIm) are the same as those in H93G-(Im), it is likely that the orientation of the methyl-substituted Im ligands are closer to that of H93G(Im) than the WT protein. Because H93G lacks a covalent linkage between the proximal ligand and the polypeptide chain, the proximal ligand orientation is determined only by its bonding and steric interactions with the heme and side chains of neighboring amino acids. The fact that the Im adopts a very different conformation in H93G than the imidazole side chain of the proximal His in WT suggests that the covalent linkage in WT restrains the ligand from a more favorable rotation and tilt. This more favorable orientation could result from the nonbonding and bonding interactions with the heme or to other stabilizing interactions in the protein pocket, such as a hydrogen bond between the Im NH and Ser 92.

The contribution from each of these interactions can be distinguished by characterization of the methyl-substituted imidazole complexes. When N-MeIm is the proximal ligand, there can be no hydrogen bond between Im NH and Ser 92. Although there are differences in the chemical shifts of the heme methyl groups, overall the hyperfine shift pattern in the spectrum of H93G(N-MeIm) is similar to that of H93G-(Im) and very different from that in WT. The observation of NOEs between ImN-CH₃ protons and protons of Ile 99 indicates that the N-CH₃ of Im is oriented away from Ser 92 in this complex. We have observed similar results in the spectra of the double mutant H93G/S92A (unpublished results). These results suggest that while the hydrogen bond between Im NH and Ser 92 may contribute somewhat to stabilizing the Im conformation, it is not the only factor.

Another difference between WT and H93G(Im) besides covalent linkage is the extra methylene group between the ring and α-carbon of His 93. 4-MeIm is a closer approximation of the histidine side chain in size and shape. If steric bulk at this position is a factor which determines the orientation of the imidazole ring, the metcyano ¹H NMR spectra H93G(4-MeIm) should be quite different from H93G-

(Im). On the contrary, the spectra of H93G(4-MeIm) and H93G(Im) are very similar (Figure 7). Thus, one can conclude that the smaller size or different shape of Im compared to histidine is not the primary factor behind the observed differences in conformation.[3]

The orientation of the imidazole ring relative to the heme plane has been the object of study in proteins and model compounds. When the proximal imidazole adopts a conformation in which Φ is 45° (Figure 1), the steric repulsion between the Im ring and the heme pyrrole nitrogens is minimized; thus, model compounds in which the proximal Im adopts this geometry have shorter N—Fe bond lengths (Collins et al., 1972; Scheidt & Lee, 1987). However, according to *ab initio* calculations (Scheidt & Chipman, 1986), bonding interactions between π orbitals of the Im and orbitals of the heme are maximized at low values of Φ. Most myoglobins and hemoglobins have $\Phi \sim 12°$, as do some porphyrin—Im model complexes (Scheidt & Lee, 1987). This observation, combined with the results of extended Hückel calculations, led Scheidt and Chipman (1986) to conclude that π-bonding determines the orientation adopted by the imidazole side chain in most Mbs and hemoglobins. The X-ray and NMR data on H93G(Im) and the NMR spectra of H93G(MeIm) suggest that the rotation of the Im plane to give a large Φ and an off-normal tilt must be the most favorable balance of bonding and steric interactions between the Im and the heme within the environment of the proximal pocket.[4] The orientation of the proximal ligand may play an important role in modulating protein function. For example, binding of NO on the distal side of H93G(Im) produces a five-coordinate NO complex, instead of the six-coordinate complex observed in WT MbNO (Decatur et al., to be published). Since the rotated Im plane should produce weaker π-bonding between Im and the heme in H93G(Im) compared to WT, this difference in conformation might have important consequences in the NO complex. In addition, the change in Im conformation may contribute to the difference observe in the kinetics of CO recombination (DePillis et al., 1994).

Kinetics of Proximal Im Exchange. The exchange of Im in the proximal pocket is slow ($\tau \sim 10$ min) and independent of the free ligand concentration. This suggests that the rate-limiting step in the ligand exchange mechanism involves either large protein structural changes, such as those which might be involved in the heme reorientation process de-

---

[3] In an earlier study, Dr. Gia DePillis in this laboratory prepared the single-site mutant H93A of human Mb for the purpose of exchanging the proximal ligand, exactly as described here for H93G(L). Large amounts of the apo-fusion protein were produced [see Varadarajan et al. (1989) for human Mb fusion protein methodology]; however, reconstitution with heme in the presence of Im failed to give a stable hemin—apoprotein complex (DePillis et al., unpublished observations, 1992). Later, Barrick (1994) adopted the strategy of randomizing the codon for H93 thereby discovering that H93G produces a stable protein in the presence of Im. The simplest interpretation of the negative result with H93A is that the total steric volume of H93A plus the added Im is greater than His, preventing stable formation of the complex. However, as shown here, 4-MeIm forms a stable complex with H93G, suggesting that the failure of H93A may be associated with the inability of this apoprotein to fold properly.

[4] The resonance Raman spectrum for deoxy H93G(Im) is not significantly different from that of deoxy WT Mb (Franzen et al., unpublished results). This suggests that stronger σ bonding made possible by closer approach of Im to the heme plane is offset by the loss of π-bonding interactions, resulting in no net change in overall Fe—Im bond strength.

scribed by La Mar and co-workers (Hauksson et al., 1990), or a large barrier to breaking the proximal bond. In either case, slow unimolecular kinetics would be expected. If protein structural reorganization is the rate-limiting process, the kinetics of ligand exchange should be independent of the nature of the distal ligand, whereas the distal ligand should modulate the exchange rate via a *trans* effect if the strength of the proximal Fe—N bond is the barrier to escape. Proximal ligand exchange is observed to be much more rapid in H93G(Im)CO (S. M. Decatur and S. G. Boxer, to be published) suggesting that breaking the Fe—N bond, rather than structural reorganization, is rate-limiting.

Relative Binding Affinities of MeIms. Since each complex H93G(L)CN has a unique fingerprint in the hyperfine-shifted region of the ^{1}H NMR spectrum, partial or incomplete exchange can be documented and quantitated. While the H93G(4MeIm)CN complex forms readily upon stoichiometric addition of 4-MeIm to H93G(Im)CN, a large excess of N-MeIm and 2-MeIm must be added to form their respective complexes. Qualitatively, the affinities of imidazoles for the proximal binding position in H93G(L)CN vary in the order Im ≈ 4-MeIm > N-MeIm > 2-MeIm. A detailed study of the absolute and relative binding constants for a wide variety of proximal ligands is currently underway (Barrick et al., to be published). Qualitatively, these observations are consistent with the structural interpretation of the ^{1}H NMR spectra. Since the spectra for H93G(4-MeIm)CN and H93G(Im)CN are so similar, there seems to be little structural reorganization upon exchange of Im for 4-MeIm, so one might expect these two ligands to bind equally well.[3] In H93G(2-MeIm)CN, the methyl group on the imidazole will lie in close proximity to the heme plane, likely lengthening the Im—Fe bond distance, as seen in model systems (Momenteau & Reed, 1994).

N-MeIm is equivalent to 4-MeIm in size and shape. In fact, on the basis of NOEs between the 1-Me or 4-Me groups and protons of Ile 99, it is likely that the two ligands adopt similar conformations in the proximal cavity. However, when N-MeIm replaces Im, there can be no hydrogen bond between the Im NH and Ser 92, and one might expect Im or 4-MeIm to bind more strongly than N-MeIm. However, as discussed above, preservation of the hyperfine-shifted methyl pattern of H93G(Im)CN in H93G(N-MeIm)CN suggests that the orientation of the Im plane is similar in the two complexes, as well as in the double mutant S92A/H93G-(Im)CN (Rickert et al., to be published). This suggests either that the loss of the hydrogen bond is balanced by an improved bonding interaction with the heme, or that the hydrogen bond is fairly weak and not a significant stabilizing factor for the Im.

ACKNOWLEDGMENT

SUPPLEMENTARY MATERIAL AVAILABLE

Six figures showing plots of $\ln[(I_\infty - I(t))/2I_\infty]$ vs τ in inversion—recovery experiments on H93G(Im)CN and for methyl resonances in H93G(N-MeIm)CN and NOE spectra of H93G(Im)CN and H93G(N-MeIm)CN (8 pages). Ordering information is given on any current masthead page.

REFERENCES

Adachi, S., Sunohara, N., Ishimori, K., & Morishima, I. (1992) *J. Biol. Chem. 267*, 12614–12621.

Adachi, S., Nagano, S., Ishimori, K., Watanabe, Y., & Morishima, I. (1993) *Biochemistry 32*, 241–252.

Alam, S. L., & Satterlee, J. D. (1994) *Biochemistry 33*, 4008–4018.

Barrick, D. (1994) *Biochemistry 33*, 6546–6554.

Carver, T. E., Rohlfs, R. J., Olson, J. S., Gibson, Q. H., Blackmore, R. S., Springer, B. A., & Sligar, S. G. (1990) *J. Biol. Chem. 265*, 20007–20020.

Collins, D. M., Countryman, R., & Hoard, J. L. (1972) *J. Am. Chem. Soc. 94*, 2066–2073.

Cutnell, J. D., La Mar, G. N., & Kong, S. B. (1981) *J. Am. Chem. Soc. 103*, 3567–3572.

DePillis, G. D., Decatur, S. M., Barrick, D., & Boxer, S. G. (1994) *J. Am. Chem. Soc. 116*, 6981–6982.

Egeberg, K. D., Springer, B. A., Martinis, S. A., Sligar, S. G., Morikis, D., & Champion, P. M. (1990) *Biochemistry 29*, 9783–9791.

Emerson, S. D., & La Mar, G. N. (1990) *Biochemistry 29*, 1545–1556.

Emerson, S. D., Lecomte, J. T. J., & La Mar, G. N. (1988) *J. Am. Chem. Soc. 110*, 4176–4182.

Hauksson, J. B., La Mar, G. N., Pande, U., Pandey, R. K., Parish, D. W., Singh, J. P., & Smith, K. M. (1990) *Biochim. Biophys. Acta 1041*, 186–194.

Inubushi, T., & Becker, E. D. (1983) *J. Magn. Reson. 51*, 128–133.

Kendrew, J. C. (1962) *Brookhaven Symp. Biol. 15*, 216–227.

La Mar, G. N. (1979) in *Biological Applications of Magnetic Resonance* (Shulman, R., Ed.) Academic Press, New York.

La Mar, G. N., & de Ropp, J. S. (1993) in *Biological Magnetic Resonance* (Berliner, L. J., & Reuben, Eds.) Vol. 12, pp 1–78, Plenum Press, New York.

La Mar, G. N., Pande, U., Hauksson, J. B., Pandey, R. K., & Smith, K. M. (1989) *J. Am. Chem. Soc. 111*, 484–491.

Lambright, D. G., Balasubramanian, S., & Boxer, S. G. (1989) *J. Mol. Biol. 207*, 289–299.

Lambright, D. G., Balasubramanian, S., Decatur, S. M., & Boxer, S. G. (1994) *Biochemistry 33*, 5518–5525.

Momenteau, & Reed, C. (1994) *Chem. Rev. 94*, 659–698.

Rajaratham, K., Qin, J., La Mar, G. N., Chiu, M. L., & Sligar, S. G. (1994) *Biochemistry 33*, 5495–5501.

Ramprassad, S., Johnson, R. D., & La Mar, G. N. (1984) *J. Am. Chem. Soc. 106*, 5330–5335.

Scheidt, W. R., & Lee, Y. J. (1987) *Struct. Bonding 64*, 1–70.

Scheidt, W. R., & Chipman, D. M. (1986) *J. Am. Chem. Soc. 108*, 1163–1167.

Smerdon, S. J., Krzywda, S., Wilkinson, A. J., Brantley, R. E., Carver, T. E., Hargrove, M. S., & Olson, J. S. (1993) *Biochemistry 32*, 5132–5138.

Takano, T. (1977) *J. Mol. Biol. 110*, 537–568.

Teale, F. W. J. (1959) *Biochim. Biophys. Acta 35*, 543.

Traylor, T., & Berzinis, A. (1980) *J. Am. Chem. Soc. 102*, 2844–2846.

Varadarajan, R., Lambright, D. G., & Boxer, S. G. (1989) *Biochemistry 28*, 3771–3781.

Walker, F. A., & Simonis, U. (1993) in *Biological Magnetic Resonance* (Berliner, L. J., & Reuben, Eds.) Vol. 12, pp 133–274, Plenum Press, New York.

Yamamoto, Y., Nanai, N., Chujo, R., & Suzuki, T. (1990) *FEBS Lett. 264*, 113–116.